Available online www.jocpr.com

Journal of Chemical and Pharmaceutical Research, 2016, 8(10):78-85

Research Article

ISSN : 0975-7384
CODEN(USA) : JCPRC5

Synthesis, DNA Binding, Cleavage and Antibacterial Studies of Nickel (II) and Copper (II) Complexes of 4-Formylpyridine N (4)-methylthiosemicarbazone

SP Mydhili[1], B Sireesha[1] and Ch Venkata Ramana Reddy[2*]

[1]*Department of Chemistry, Nizam College, Hyderabad, India*
[2]*Department of Chemistry, Jawaharlal Nehru Technological University Hyderabad, Hyderabad, India*

ABSTRACT

Binary Ni(II) and Cu(II) complexes with 4-Formylpyridine N(4)-methyl thiosemicarbazone (H4FP4MT) were prepared and characterized by various spectro-analytical techniques: elemental analyses, molar conductance, magnetic susceptibility measurements, LC-MS, TGA, IR, UV-visible and ESR spectra. Elemental analyses, LC-MS and TGA studies reveal the composition as ML_2 for nickel and $(ML)_2$ for copper complexes. Interaction of the complexes with CT-DNA, investigated by electronic absorption titrations, fluorescence quenching studies and viscosity measurements suggest partial intercalation of nickel and intercalation of copper complexes with DNA. These complexes also promote hydrolytic cleavage of plasmid pBR322. Antibacterial activity of the ligand and metal complexes were studied against gram positive and gram negative bacterial strains and found to be active.

Keywords: Bidentate ligand; Distorted octahedral geometry; CT-DNA; antibacterial nature

---

INTRODUCTION

Thiosemicarbazones have emerged as an important class of ligands with nitrogen and sulphur donor atoms. Thiosemicarbazones became a topic of interest in research field due to their broad spectrum of biological activity such as antitumour, antifungal, antibacterial, anticancer etc [1-4]. Presence of an additional potential bonding site along with bulky groups at the N(4) position of the thiosemicarbazone moiety significantly enhances biological activity [5,6]. Pyridine-2-carboxaldehydethiosemicarbazone was first among α-(N-) thiosemicarbazones to be reported carcinostatic due to its ability to inhibit biosynthesis of DNA [7]. In view of the importance of thiosemicarbazone derivatives, the present communication reports the synthesis, characterization, DNA binding, cleavage and anti-bacterial activities of Ni(II) and Cu(II) complexes of 4-FormylpyridineN(4)-methyl thiosemicarbazone (H4FP4MT).

EXPERIMENTAL SECTION

All the chemicals used were of AR grade (Sigma-Aldrich). LC-MS of the ligand and its complexes were recorded on LCMS 2010A, Shimadzu spectrometer, elemental analysis was done on Thermo Finnigan/Eager 300 for EA 11120. Molar conductivity of the complexes ($1x10^{-3}$M) was measured using Digisun (909) digital conductivity meter. Thermo gravimetric analyses of the complexes were carried on TG balance TA Model: Q/50 in the temperature range of 0°C to 1000°C with a ramp of 20°C per min. IR spectra in KBr were recorded on Schimadzu (Prestige-21) FTIR spectrometer, ^{1}H-NMR (with D_2O exchange) and ^{13}C-NMR of the ligand were recorded on Varian 400MHz NMR spectrometer. ESR spectrum of copper complex was recorded on Jeol, JES – FA 200 ESR spectrometer and UV spectra in DMSO were recorded on Schimadzu UV 2450 spectrophotometer. Fluorescence spectra were recorded on RF-5301-PC Schimadzu spectro fluorimeter and Ostwald's viscometer was used for viscosity studies. Anti-bacterial activity was studied following Kirby-Bauer disc diffusion method in sterile nutrient agar medium.

Synthesis of ligand, L (H4FP4MT)

H4FP4MT (Figure 1) was synthesized by stirring equimolar (0.01M) solutions of N(4)-methyl thiosemicarbazide and 4-formyl pyridine at room temperature for one hour. The progress of the reaction was monitored by TLC. Pale cream coloured product formed was filtered, washed with water, dried and recrystallised from ethanol.

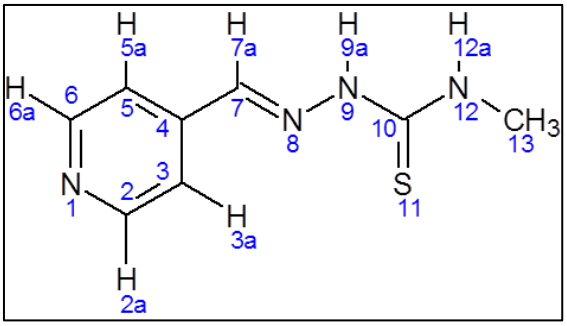

Figure 1: 4-Formylpyridine N(4)-methyl thiosemicarbazone

Yield: 90%; colour: pale cream; m.p. 213°C-215°C; Elemental Anal. Calc. for $C_8H_{10}N_4S$: C 49.42%, H 5.14%, N 28.82%; Found: C 49.65%, H 5.06%, N 28.76%; IR (υ,cm^{-1}; KBr): 3280 υ(N_4-H), 3142 υ(N_3-H), 1597 υ(C=N), 1257 υ(N-CS-N), 985 υ(N-N), 819 υ(C=S); ^{1}H NMR (DMSO, ppm): δ11.76 (s, 1H, N_3-**H**), δ8.7 (d, 1H, N_4-**H**), δ8.58 (d, 2H, Ar-**H**), δ7.75 (d, 2H, Ar-**H**), δ7.97 (1H, s, **H**-C=N), δ3.01(s,3H, N-C**H**$_3$); ^{13}C NMR (DMSO-d_6, δ/ppm): 141.9 (C_2, C_6), 121.5 (C_3, C_5), 139.2 (C_4), 150.4 (C_7), 178.5 (C_{10}), 31.3(C_{13}). UV-visible in DMSO, λ_{max}/nm: 330, 249.5; APCI(+) MS: m/z 195 $[M+1]^+$.

Synthesis of complexes

To the hot methanolic solution of H4FP4MT (L) corresponding aqueous metal ion(M) $NiCl_2$/ $CuCl_2$ solutions in 1:2 (M:L) molar ratio were added and refluxed for 5-6 hours. pH of the solution was adjusted by addition of few drops of methanolic ammonium hydroxide solution. Solid complexes formed were filtered under hot condition, washed with hot methanol, water and with petroleum ether and finally dried in vacuum [8].

$[Ni\ (C_8H_9N_4S)_2\ (H_2O)_2]$ (1)

Colour: yellow; m.p. > 300°C; Anal. Calculated for $C_{16}H_{22}NiN_8S_2O_2$: C 39.89%, H 4.57%, N 23.27%; Found: C 40.38%, H 4.51%, N 23.96%; IR (υ_{max},cm^{-1}; in KBr): 3311 υ(N_4-H), 1612,1580 υ(C=N), 1246 υ(N-CS-N),1012 υ(N-N); UV-visible in DMSO, λ_{max}/nm: 424.5, 470, 883.5; APCI(-)MS *m/z*: 480$[M-1]^+$

$[Cu\ (C_8H_{10}N_4S)(Cl)_2(H_2O)_2]_2$ (2)

Colour: brown; m.p. > 300°C; Anal. Calculated for $C_{16}H_{28}Cl_4Cu_2N_8S_2O_4$: C 26.31%, H 3.83%, N 15.35%; Found: C 27.15%, H 3.76%, N 15.63%; IR (υ_{max},cm^{-1}; in KBr): 3346 υ(N_4-H), 1597 υ(C=N), 1014 υ(N-N), 1245 υ(N-CS-N); UV-visible in DMSO, λ_{max}/nm: 410, 782.5, 970; APCI(-)MS m/z: 727$[M-2]^+$

DNA Binding Studies

Electronic absorption Titrations

CT-DNA solution was prepared in 5mM TrisHCl-50mM NaCl, pH 7.2 buffer. DNA concentration per nucleotide was calculated as reported in literature [9,10]. Stock solutions of the samples in DMSO were diluted to 20µM using tris HCl buffer. Absorption titrations were carried out with increasing concentrations from 0-210µL of CT-DNA, [DNA] =153µM. The test solutions were incubated for ten minutes before each recording. DNA solution was added to both test and reference solutions to eliminate the absorption of CT-DNA itself. From the titration data, binding constant (K_b) was calculated from the equation

$$[DNA] / (\varepsilon_a-\varepsilon_f) = [DNA] / (\varepsilon_b-\varepsilon_f) + 1/ K_b\ (\varepsilon_b-\varepsilon_f) \qquad (1)$$

Where, [DNA] is the concentration of CT-DNA in base pairs, ε_a, ε_b, ε_f are extinction coefficients of apparent, bound and free complex respectively. Ratio of slope to intercept from the plot of [DNA] vs [DNA]/(ε_a- ε_f) gives binding constant (K_b) of the complex[9,10].

Fluorescence quenching studies

Competitive binding experiments were carried out in tris HCl buffer with [DNA]/[EB] = 1 and increasing concentrations from 0-400µL of complex, [complex]=50µM. The fluorescence spectra of ethidium bromide

(EB) were measured at excitation wavelength of 520nm and the emission range was set between 530 and 770nm. Spectra were analyzed as per classical Stern-Volmer equation

$$I_0/I = 1 + K_{sv}\, r \qquad (2)$$

where I_0 and I are the fluorescence intensities in the absence and presence of the quencher, K_{sv} is the linear Stern-Volmer quenching constant, r is the ratio of the total concentration of complex to that of DNA. K_{sv} for the complexes were calculated from linear fit plot of I_0/I vs r [11,12].

Viscosity studies

Relative viscosity measurements were carried out using an Ostwald's viscometer maintained at a constant temperature of 27.0 (±0.1)°C in a thermostatic bath. Flow time was measured with a digital stopwatch by increasing concentrations 0-100µL of the complex, [complex]=50µM stock. Flow time was measured in triplicate and was averaged. Data were presented as $(\eta-\eta_0)^{1/3}$ vs ratio of the concentration of the compound to CT-DNA, where η is the viscosity of CT-DNA in the presence of the complex and η_0 is the viscosity of CT-DNA alone. Viscosity values were calculated from the observed flow time of CT-DNA containing solutions corrected from the flow time of buffer alone (t_0), $\eta=(t-t_0)/t_0$ [11,13].

DNA cleavage studies

pBR322 plasmid DNA dissolved in buffer containing 10mM Tris-HCl (pH 7.5), 1mM EDTA and 0.1% sodium azide was used. TAE buffer (pH 8.0; 40mM Tris base, 20mM acetic acid and 1mM Na_2EDTA) was used for gel electrophoresis. 3µL of super coiled pBR322 DNA (100ng/µL) was treated with the complexes (15-45µM), incubated for 1hour at 37^{O}C and loaded onto a 0.8% agarose gel after addition of 1µL loading buffer (0.25% bromo phenol blue). This was subjected to electrophoresis at 60V for 2hours until bromophenol blue had travelled through 75% of the gel. Later, gel was stained with EB and then destained in sterile distilled water. The plasmid bands were visualized under transilluminator and photographed [11].

Antibacterial studies

Biological activity of all the complexes was tested by disc diffusion method [14]. 0.10mL of test bacteria [gram positive-Staphylococcus aureus and Bacillus subtilis and gram negative -Escherichia coli and Klebsiella pneumonia] was spread over the surface of nutrient agar. Sterile discs of 5mm diameter dipped in DMSO solutions of test samples are placed at equidistance. The potency of the samples tested was 1000µg/disc. Capacity of the disc is 5µL of the sample. DMSO was taken as control, which has no antibacterial activity. Gentamycin was used as standard. Zone of inhibition was recorded after incubation for 24hrs at 37°C. All these tests were made in triplicate and are averaged.

RESULTS AND DISCUSSION

Characterization of complexes

Metal complexes were coloured, crystalline and stable .They are soluble in DMSO and DMF. Elemental analyses, mass spectral data and TGA confirm the formation of ML_2 for complex(**1**) and $(ML)_2$ for complex(**2**). Low molar conductivity values (0-12 Scm^2M^{-1}) indicate their nonelectrolytic nature [15]. Presence of chloride ions in complex(**2**) was established from Volhard's test [16].

Liquid chromatograms

Liquid chromatograms of the complexes showed single peak with retention time of 0.636 and 0.646 min respectively indicate their purity.

Mass spectra

APCI (-) mass spectrum of complex(**1**)showed a molecular ion peak at m/z 480. Peak at m/z 444 is by loss of water molecules and also reveals 1:2(M:L) nature of complex. A peak at m/z 386 corresponds to two ligand moieties in the complex. In the APCI (-) mass spectrum of complex(**2**), peak at m/z 727 indicate dimeric nature of this complex. Peaks at m/z 515 and m/z 257 show 2L:2M and L:M of the complex respectively. Peaks at m/z 386 and m/z 126 indicate presence of two ligand moieties and two metal ions in the complex.

Thermogravimetric analysis

In the thermogram of complex(**1**), weight loss from 230°C to 280°C is due to loss of coordinated water molecules. Gradual decomposition in two steps from 280°C to 791°C corresponds to decomposition of ligand moiety. The residue (24.53%) at 791°C corresponds to metal oxide and complete analysis provide evidence for 1:2 (M:L) composition of the complex. Thermogram of complex(**2**), showed three steps decomposition. Gradual weight loss from 180°C to 225°C corresponds to loss of coordinated water molecules. Sudden decrease till

350°C (43%) and gradual weight loss till 940°C (7.15%) correspond to decomposition of ligand moiety. Residue (33%) correspond to 1:2 (M:L). Thermograms of the complexes are presented in Figure 2.

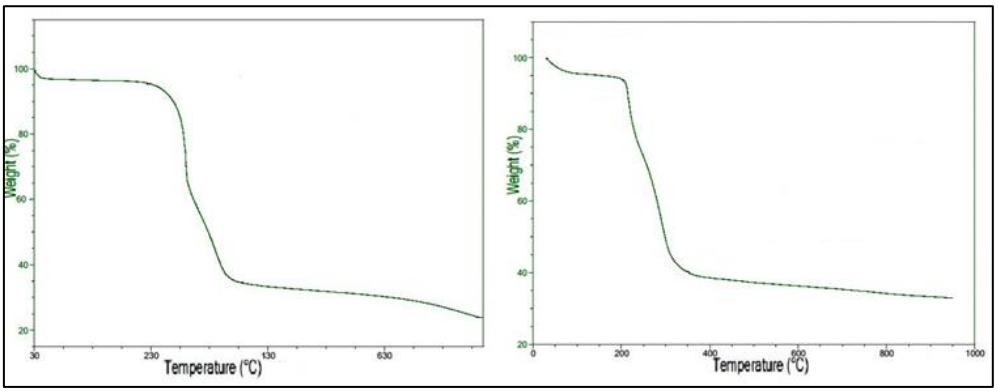

Figure 2: Thermograms of complexes(1,2)

IR spectral data

In IR spectra of the complexes (Table 1, Figure 3), υC=N shifted towards lower frequency suggest the coordination of azomethine nitrogen with metal ions, which is also supported by an increase in υN-N of the ligand [17, 18]. υ(N-CS-N) shifted towards lower frequency suggesting the coordination of sulphur [19, 20]. From the far IR region of the spectra, there is evidence for the presence of (M-N), (M-S), (M-Cl) and (M-OH_2) bands in the complexes. Analysis of IR spectral data shows that the ligand is bidentate with azomethine nitrogen and thiolate/thione sulphur as potential donor sites forming five membered chelates with the metal ions.

Table 1: IR Spectral data (KBr, cm^{-1})

Compound	υ(C=N)	υ (N-CS-N)	υ (N-N)
H4FP4MT(**L**)	1597	1257	985
Complex(**1**)	1,61,21,580	1246	1012
Complex(**2**)	1597	1245	1014

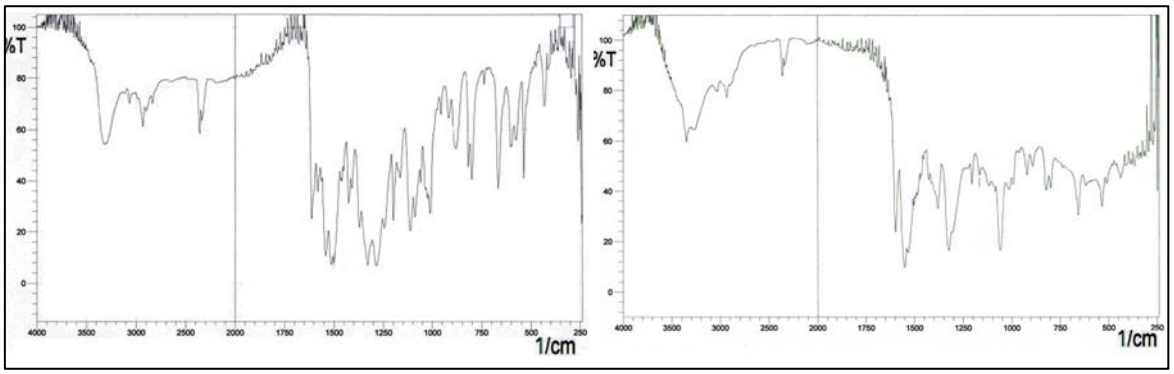

Figure 3: IR Spectra of complexes(1,2)

Electronic spectra and magnetic moments

From the electronic spectrum of complex(**1**), three d-d transitions at 883.5nm [υ_1, $^3A_{2g} \rightarrow {}^3T_{2g}$ (F)], 470nm [υ_2, $^3A_{2g} \rightarrow {}^3T_{1g}$ (F)] and 424.5nm [υ_3, $^3A_{2g} \rightarrow {}^3T_{1g}$ (P)] reveal distorted octahedral geometry of the complex [21] . In electronic spectrum of complex(2), three bands at 970nm [υ_1, $^2B_{1g} \rightarrow {}^2A_{1g}$], 782.5nm [$\upsilon_2$, $^2B_{1g} \rightarrow {}^2B_{2g}$], 410nm [$\upsilon_3$, $^2B_{1g} \rightarrow {}^2E_{1g}$] confirms distorted octahedral geometry [1, 21].

ESR spectra

The nuclear spin (I) of copper is 3/2 and this led to further splitting of signal to a quartet at liquid nitrogen temperature. The hyperfine ESR spectrum of complex(2) in DMSO (Figure 4) showed well resolved peaks in g∥ (2.5283, 2.1597) and $g_{\perp}$ (2.04712- 1.8641).The greater values of g∥ suggest distortion from regular octahedral geometry and anisotropic environment around copper ion. Both g∥, $g_{\perp}$ >2.0023 indicates that the unpaired electron is localized in d_{x2-y2} orbital of the metal ion [22].

Magnetic moment

The magnetic moment value (3.08BM) calculated for the complex(1) corresponds to two unpaired electrons and is an outer orbital complex, with distorted octahedral geometry. From the magnetic measurements of complex(**2**), the magnetic moment was found to be 2.44BM, which suggests the presence of one unpaired electron as known from ESR studies.

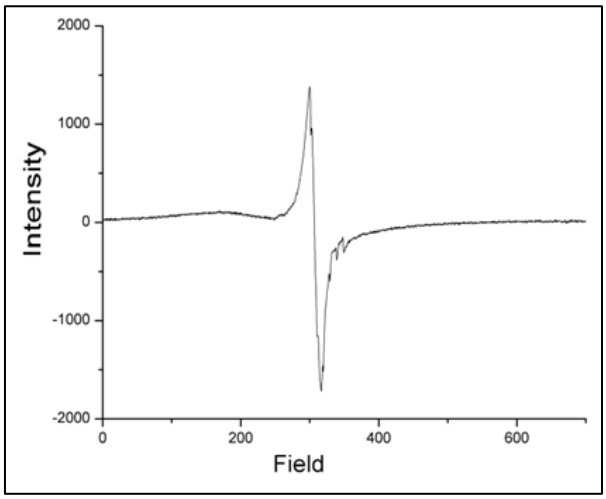

Figure 4: ESR spectrum of complex(1)

From the spectra and analytical data, the proposed structures of the complexes are shown in Figure 5.

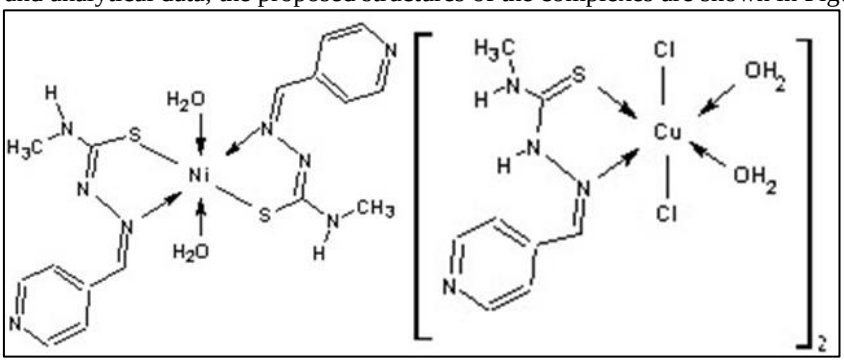

Figure 5: Proposed structures of complexes(1,2)

DNA Binding Studies

Electronic absorption spectra

Electronic absorption spectroscopy is widely employed to study the binding interactions of the metal complexes with DNA. Hypochromism is observed due to intercalation involving strong $\pi \rightarrow \pi^*$ stacking interactions between the aromatic chromophore and the base pairs of DNA [23].

In the present study both the complexes showed hypochromism (Figure 6). This infers that these complexes intercalate with base pairs of the CT-DNA. The intrinsic binding constant (K_b) calculated from the plots of [DNA] vs [DNA]/(ε_a-ε_f)) for complexes(1,2) are $4.0 \times 10^4 M^{-1}$ and $1.0 \times 10^5 M^{-1}$ respectively. The greater value of K_b indicate greater interactions of complex(**2**) with DNA.

Free energy of DNA-complex system can be calculated using equation

$$\Delta G = -RT \ln K_b \qquad (3)$$

Where, ΔG is Gibb's free energy in kJ mol^{-1}, R is the gas constant (8.314 $JK^{-1}mol^{-1}$), T is temperature in Kelvin and K_b is the binding constant of DNA-complex [23].

Free energy change gives a measure of the spontaneity of the binding of complex to DNA. Calculated free energies of complexes(1,2) were -27.14kJmol^{-1} and -29.4kJmol^{-1} respectively. The results indicate that the complex(2) binds to CT-DNA more spontaneously than complex(1).

Fluorescence quenching studies

EB is a conjugate planar molecule with very weak fluorescence intensity which increases greatly when intercalated into the base pairs of double-stranded DNA. When EB is free from DNA, the fluorescence of DNA-EB complex is quenched. Therefore EB can be used as a probe for DNA structure detection. The complexes do not show fluorescence in the spectral region studied, either free or bound to DNA, and does not quench the fluorescence of EB in the absence of DNA under experimental conditions. The fluorescent emission of EB bound to DNA in the absence and the presence of complex is shown in Figure 7. The emission intensity at 609nm of the DNA-EB system decreased with increasing the complex concentration. This indicates that the complexes compete with EB in binding to DNA [11].

The fluorescence quenching curves are in good agreement with the linear Stern–Volmer equation, which proves that both the complexes bind to DNA. From the linear fit plot of I_0/I vs r, the K_{sv} values for complexes(1,2) are 0.09 and 0.1 respectively.

Based on the K_{sv} values it was determined that the binding strength complex(2) greater than complex(1).

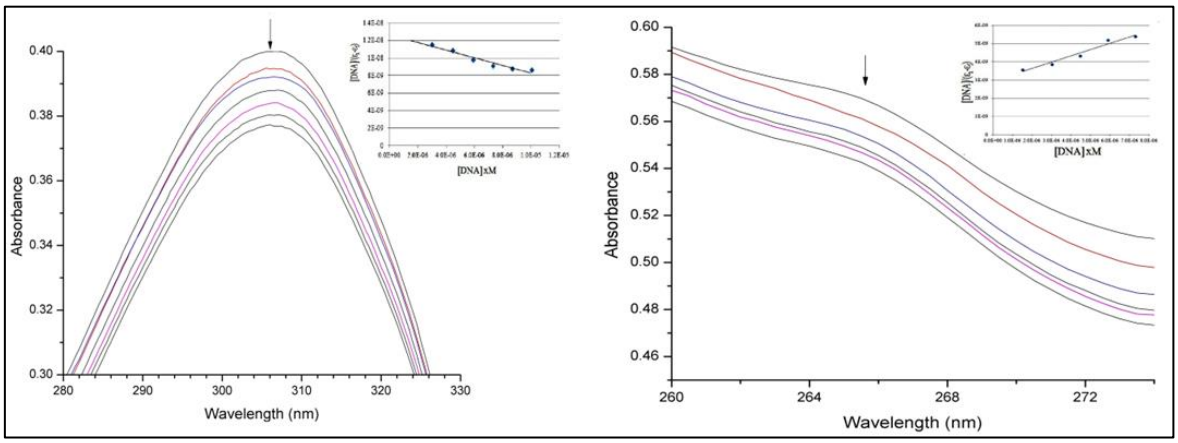

Figure 6: Absorption spectra of complexes(1,2) [20µM] in increasing concentrations (0-210µL) of CT-DNA, [DNA]=153µM [Inset: Plots of [DNA] vs [DNA] / (ε_a- ε_f)]

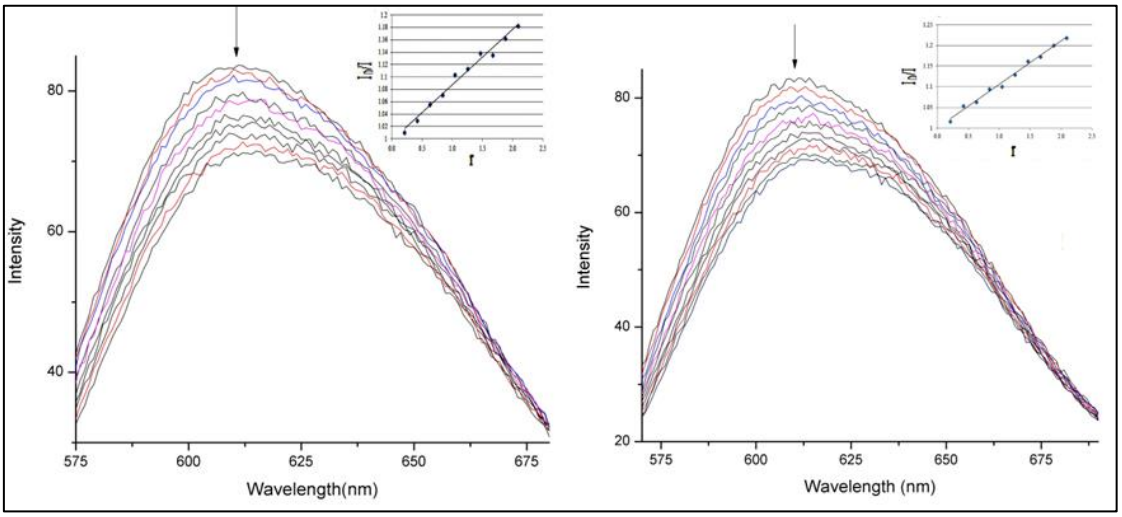

Figure 7: Emission spectra of EB –DNA, in increasing concentrations (0-400µL) of complexes, [complex]=50µM, [DNA]=20µM (Inset: Stern–Volmer quenching curves)

Viscosity studies

Though spectroscopic experiments provide information about the nature and strength of metal complex-DNA interaction, does not give sufficient information about binding mode. Hydrodynamic measurements like viscosity and sedimentation are considered to be least ambiguous and most crucial test of metal complex-DNA binding in solution in the absence of crystallographic data.

Intercalative mode of binding must lengthen the DNA helix, as base pairs are separated to accommodate the binding molecule. This leads to increase in the viscosity of DNA.

In contrast, a partial intercalation of ligand could bend (or kink) the DNA helix, decrease its effective length and inturn its viscosity [24].

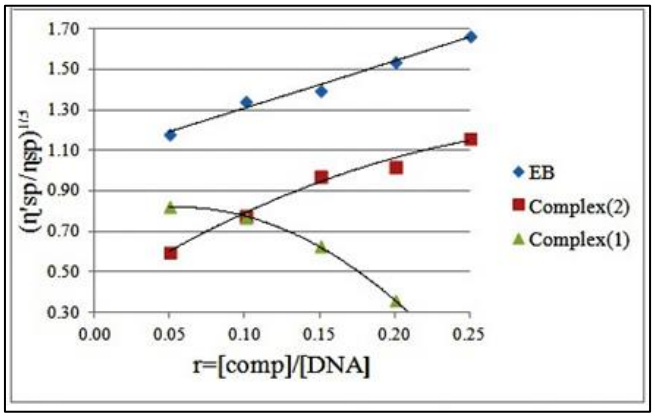

Figure 8: Effect of increasing amount of EB and complexes(1,2)on the relative viscosity of CT-DNA at 27.0 (±0.1)°C

From the Figure 8, it is evident that the relative viscosity of the complex(**1**) decreases indicating partial intercalation with CT-DNA while increase in viscosity of complex(**2**) indicate intercalation.

DNA Cleavage studies

Super coiled (SC) plasmid DNA, commonly seen in bacteria cells, is a cyclic super coiled double strand made up of several thousand base pairs. This is an important substrate for hydrolytic cleavage. Metal ions in the complexes serve as Lewis acids to activate the phospho-diester links for nucleophilic attack and metal coordinated water species acts as a nucleophile. When DNA is subjected to electrophoresis, the intact SC form migrates faster. When scission occurs to complex, SC form will relax to nicked (NC) form. Cleavage of both types of strands leads to linear form which migrates between SC and NC forms. This is because shorter molecules migrate more easily through the pores of the gel [25]. In the present investigation, considerable intensity of nicked forms suggests their hydrolytic cleavage activity (Figure 9).

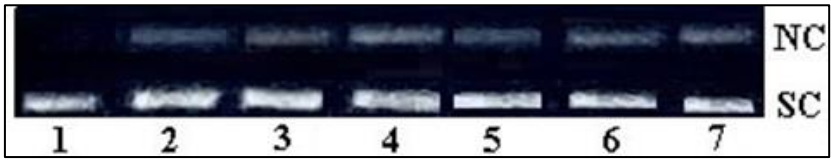

Figure 9: Changes in the agarose gel electrophoresis pattern of pBR322 plasmid DNA through hydrolytic cleavage: (1) DNA alone; (2,3,4) DNA + complex1 (15,30,45µM); (5,6,7) DNA + complex2 (15,30,45µM)

Antibacterial studies

Activity of H4FP4MT and its complexes have been tested on both gram positive and gram negative bacteria. From the table 2, it is evident that the ligand can inhibit the growth of gram positive bacteria. Both the complexes are active against gram positive and gram negative bacteria. The complex(2) exhibit more activity than ligand and complex(1). This can be due to partial sharing of positive charge of the metal ion with the donor atoms of the ligand leading to π electron cloud delocalization over the chelated ring. Hence the lipophilicity of the metal complex enhances and favours its penetration into bacterial cell membranes and hinders the growth of the bacteria [14].

Table 2. Anti bacterial activities of H4FP4MT and complexes (zone of inhibition)

Compound	*S.aureus*	*B.subtilis*	*E. coli*	*K.pneumoniae*
H4FP4MT	6mm	6mm	-	-
Complex(1)	3mm	4mm	5mm	6mm
Complex(2)	9mm	15mm	6mm	7mm

CONCLUSION

H4FP4MT acts as bidentate ligand and forms distorted octahedral metal complexes with Ni(II) and Cu(II) ions. DNA binding studies suggest partial intercalation of Ni(II) complex and intercalative binding of Cu(II) complex. Both the complexes promote hydrolytic cleavage of plasmid pBR322. Antibacterial studies suggests greater activity of Cu(II) complex over the ligand and Ni(II) complex.

ACKNOWLEDGEMENTS

The authors are thankful to Osmania University, Hyderabad and Loyola Academy Degree & PG College, Secunderabad for providing necessary facilities to carry out this work.

REFERENCES

[1] S Chandra; S Raizada; M Tyagi; PK Sharma. *Spectrochim. Acta A.*, **2008**, 69, 816-821.
[2] SA Elsayed; AM El-Hendaway; SI Mostafa; IS Butler. *Inorg. Chim. Acta*., **2010**, 363, 2526-2532.
[3] J Wiecek; D Kovala-Demertzi; Z Ciunik; J Wietrzyk; M Zervou; MA Demertzis. *Bioinorg. Chem. Appl*., **2010,** Article ID 718606.
[4] EN Nfor; SN Esemu; GA Ayimele; EA Eno; GE Iniama; OE Offiong. *B. Chem. Soc. Ethiopia*., **2011,** 25, 361-370.
[5] SK Jain; BS Garg; YK Bhoon. *Spectrochim. Acta A*., **1986**, 42, 959-968.
[6] ME Hossain; M N Alam; J Begum; MA Ali; M Nazimudhin; FE Smith; RC Hynes. *Inorg. Chim. Acta*., **1996**, 249, 207-213.
[7] PF Raphel; E Manoj; MRP Kurup. *Polyhedron*., **2007**, 26, 818-828.
[8] B Sireesha; Ch Sarala Devi; Rafeeq Mohiuddin; M RamReddy. *J. Indian Chem Soc*., **1999,** 76, 498-499.
[9] HuiluWu; Tao Sun; Ke Li; Bin Liu; Fan Kou; Fei Jia; Jingkun Yuan; Ying Bai. *Bioinorg. Chem. Appl*., **2012**, Article ID 609796.
[10] RK Sahu; F Khan; Kush Nayak. *Chemistry and Materials Research*., **2015**, 7, 40-47.
[11] Cheng-Yong Zhou; Jing Zhao; Yan-Bo Wu; Cai-Xia Yin; Pin Yang. *J. Inorg. Biochem*., **2007**, 101, 10-18.
[12] D Kannan; MN Arumugham.. *International Journal of Research in Controlled Release*., **2012**, 2, 10-17.
[13] P Jayaseelan; E Akila; M Usha Rani; R Rajavel.. *Journal of Saudi Chemical Society.*, **2013,** http://dx.doi.org/10.1016/j.jscs.2013.07.001
[14] S Chandra; S Parmar; Y Kumar. *Bioinorg. Chem. Appl*., **2009**, Article ID 851316, 6 pages.
[15] R Aman; G Matela; Chetan Sharma; Smita Chaudhary. *Arabian Journal of Chemistry*., **2015**, 8, 698-705.
[16] AI Vogel. A Text Book of Qualitative Inorganic Analysis, 3rd Edition. Longman, London. **1968**.
[17] G Kanagaraj; GN Rao. *Polyhedron*., **1993**,12, 383-387.
[18] DX West; H Beraldo; AA Nassar. *Transit. Metal. Chem*., **1999**, 24, 25-28
[19] RL de Lima; LR de Souza Teixeira; TMG Carneiro; H Beraldo. J. Braz. *Chem. Soc*., **1999**, 10, 184-188.
[20] H Beraldo; R Lima; LR Teixeira; AA Moura; DX West. *J Mol.Struct*., **2001**, 559, 99-106.
[21] ABP Lever, Inorganic Electronic Spectroscopy, 2nd Edition, Elsevier Science Publishers, Amsterdam, **1984**.
[22] B Anupama; Ch Venkata.Ramana Reddy; CG Kumari., *Chem Sci Trans*., **2013**, 2(2), 461-466.
[23] K Karami; Z Shirani-Sarmazeh; M Hosseini-Kharat; J Lipkowski; M Saeidifar; *J. Photochem. Photobiol B*., **2015**, 144, 11-19.
[24] T Topala; A Bodok; L Oprean; R Oprean, *Farmacia*., **2014**, 62, 1049-1061.
[25] PR Reddy; A Shilpa. *Indian Journal of Chemistry*., **2010**, 49A, 1003-1015.